Supporting information:

Ring-extended Carbazole Modification to Activate Efficient Phosphorescent OLED Performance of Traditional Host Materials

Zhen-Long Tu,[*ab#] Li-Yuan Hu,[a#] Jun-Yi Wang,[a#] Cong Wang,[a] Xunwen Xiao,[*a,d] Xu-Feng Luo,[*a]

[a] *College of Material Science and Chemical Engineering, Ningbo University of Technology, Ningbo 315211, P. R. China.*

[b] *School of Materials and Energy, University of Electronic Science and Technology of China, Chengdu 611731, P. R. China.*

Z.-L. Tu, L.-Y. Hu and J.-Y. Wang contributed equally to this work.

General Information

All reagents and chemicals were purchased from commercial sources and used without further purification. All reactions were performed under nitrogen atmosphere unless otherwise stated. ^{1}H NMR spectra were recorded in dichloromethane-d_2 ($CDCl_3$) on Bruker 500 MHz at room temperature. ^{13}C NMR spectra were recorded in $CDCl_3$ on Bruker 500 MHz MHz NMR spectrometer. High resolution mass spectra (HRMS) were measured by Thermo Scientific LTQ Orbitrap XL mass spectrometer. UV-vis absorption spectra were recorded on Cary 60 spectrometer (Agilent Technologies). PL spectra and phosphorescent spectra were recorded on a Hitachi F-4600 fluorescence spectrophotometer. Differential scanning calorimetry (DSC) was performed on a TA DSC 2010 unit at a heating rate of 5^{o}C min^{-1} under nitrogen. The glass transition temperatures (T_g) were determined from the second heating scan. Thermogravimetric analysis (TGA) was performed on a TA SDT 2960 instrument at a heating rate of 10^{o}C min^{-1} under nitrogen. Temperature at 5% weight loss was used as the decomposition temperature (T_d). Cyclic voltammetry (CV) was carried out on a CHI600 voltammetric analyzer at room temperature with ferrocenium-ferrocene (Fc^{+}/Fc) as the external standard. The oxidative scans were performed using 0.1 M *n*-Bu_4NPF_6 ($TBAPF_6$) in deoxygenated with nitrogen dichloromethane as the supporting electrolyte. A conventional three-electrode configuration consisting of a Pt-wire counter electrode, an Ag/AgCl reference electrode, and a Glassy-Carbon working electrode was used. The cyclic voltammograms were obtained at a scan rate of 0.1 V s^{-1}. The HOMO and LUMO levels can be calculated by using the following equations: $LUMO = -(E^{red} - E_{Fc/Fc+} + 4.8)$, $HOMO = -(E^{ox} - E_{Fc/Fc+} + 4.8)$. E^{red} /Eox were calculated from CV data. The optimization of the ground state configuration is based on the density functional theory DFT/ B3LYP/ 6-31G(d) method.

Device Fabrication and Measurement

All devices were evaporated on the glass covered by pattern-ITO layer (135 nm, 15 Ω square^{-1}) under vacuum of 3 × 10^{-6} Torr. The active area of each device is 0.09 cm^2. The ITO substrates were cleaned by acetone, ethanol and deionized water in the ultrasonic machine for 15 min each, respectively. Before evaporation, the dried ITO surface was treated by UV-ozone for 15 min. The deposition rate was controlled at 2

Å s^{-1} for other organic layers and 6-8 Å s^{-1} for Al anode. The current–voltage characteristics were measured with a computer controlled Keithley 2400 source meter. Electroluminescence spectra were collected by using a photonic multichannel analyzer PMA-12 (Hamamatsu C10027-01). The external quantum efficiency of the devices was obtained by measuring the light intensity in the forward direction by using an integrating sphere (Hamamatsu A10094). All the measurements were carried out in ambient.

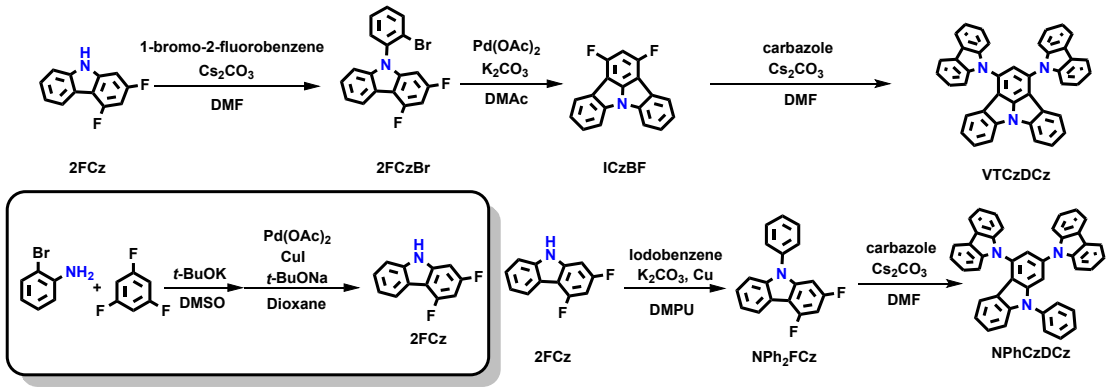

Scheme S1. Molecule structures and synthesis routes of NPhCzDCz and VTCzDCz.

Synthesis and characterization

Preparation procedure for 2FCz and ICzBF:

The synthesis routes of 2FCz and ICzBF as key precursors refer to our previous work (*Angew. Chem. Int. Ed*. **2022**, *61*, e202209984).

Preparation procedure for NPh_2FCz:

A mixture of 2FCz (2.00 g, 9.85 mmol), Iodobenzene (2.41 g, 11.82 mmol), potassium carbonate (2.04 g, 14.78 mmol) and copper powder (320.00 mg, 5.00 mmol) in 20 mL DMPU under nitrogen was stirred at 200°C for 24 h. After cooling down to room temperature, the product was extracted with dichloromethane (3 × 30 mL) and washed with water. The combined organic phase was dried over anhydrous sodium sulfate and then concentrated under reduced pressure. The crude product was purified by column chromatography on silica gel using 1:5 dichloromethane/petroleum as eluent to afford a white solid (1.82 g, 66%).^{1}H NMR (500 MHz, $CDCl_3$) δ 8.23 (d, J = 7.7 Hz, 1H), 7.69 – 7.62 (m, 2H), 7.58 – 7.52 (m, 3H), 7.46 – 7.41 (m, 1H), 7.39 – 7.32 (m, 2H), 6.88 (dd, J = 9.4, 1.9 Hz, 1H), 6.77 (td, J = 9.9, 2.0 Hz, 1H). ^{13}C NMR (126 MHz, $CDCl_3$) δ 162.68 (d, J = 12.4 Hz), 160.74 (d, J = 12.4 Hz), 157.07 (d, J = 15.2 Hz), 142.72 (s), 141.05 (s), 136.93 (s), 130.11 (s), 128.20 (s), 127.10 (d, J = 16.2 Hz), 125.79 (s), 122.49 (d, J = 3.3 Hz), 120.96 (s), 120.53 (s), 109.69 (s), 95.87 (s), 95.66 (d, J = 4.9 Hz), 95.46 (s), 93.00 (d, J = 4.1 Hz), 92.78 (d, J = 4.1 Hz).

Preparation procedure for NPhCzDCz:

carbazole (2.00 g, 11.98 mmol) and Cs_2CO_3 (4.68 g, 14.37 mmol) were dissolved in DMAC (50 mL) at room temperature. After stirring for 30 min, the NPh_2FCz (1.60 g, 5.7 mmol) was added to the solution. The mixture was stirred at 190 ºC for 24 h. After

cooling to room temperature, the reaction mixture was poured into a large amount of water. The product was extracted with dichloromethane, and the combined organic layer was dried over anhydrous $MgSO_4$. After filtration and evaporation, the crude product was purified by column chromatography on silica gel (PE/DCM= 8/1, v/v) to get the NPhCzDCz as white solid (yield = 2.2 g, 68%). ^{1}H NMR (500 MHz, $CDCl_3$) δ 8.29 (d, *J* = 7.5 Hz, 2H), 8.16 (d, *J* = 7.7 Hz, 2H), 7.76 (d, *J* = 1.6 Hz, 1H), 7.67 (dt, *J* = 10.1, 4.4 Hz, 5H), 7.54 (dd, *J* = 17.4, 7.8 Hz, 3H), 7.38 (dddd, *J* = 28.8, 20.4, 12.9, 7.3 Hz, 12H), 6.91 (t, *J* = 7.5 Hz, 1H), 6.70 (d, *J* = 7.9 Hz, 1H). ^{13}C NMR (126 MHz, $CDCl_3$) δ 141.07 (s), 140.90 (s), 130.28 (s), 128.34 (s), 127.33 (s), 126.71 (s), 126.15 (d, *J* = 10.9 Hz), 123.51 (d, *J* = 16.1 Hz), 123.10 (s), 120.72 (d, *J* = 9.9 Hz), 120.63 – 120.03 (m), 119.14 (s), 110.53 (s), 109.71 (d, *J* = 3.5 Hz), 108.38 (s), 1.04 (s).

Preparation procedure for VTCzDCz:

carbazole (2.00 g, 11.98 mmol) and Cs_2CO_3 (4.68 g, 14.37 mmol) were dissolved in DMAC (50 mL) at room temperature. After stirring for 30 min, the ICzBF (1.66 g, 6.00 mmol) was added to the solution. The mixture was stirred at 190 ºC for 24 h. After cooling to room temperature, the reaction mixture was poured into a large amount of water. The product was extracted with dichloromethane, and the combined organic layer was dried over anhydrous $MgSO_4$. After filtration and evaporation, the crude product was purified by column chromatography on silica gel (PE/DCM= 8/1, v/v) to get the VTCzDCz as a white solid (yield = 2.8 g, 84%).^{1}H NMR (500 MHz, $CDCl_3$) δ 8.28 (d, *J* = 7.6 Hz, 4H), 8.03 (d, *J* = 8.0 Hz, 2H), 7.97 (s, 1H), 7.60 – 7.54 (m, 6H), 7.49 – 7.43 (m, 4H), 7.43 – 7.37 (m, 4H), 7.17 – 7.11 (m, 2H), 7.05 (d, *J* = 7.7 Hz, 2H). ^{13}C NMR (126 MHz, $CDCl_3$) δ 146.26 (s), 140.77 (s), 139.24 (s), 131.02 (s), 127.99 (s), 127.31 (s), 126.28 (s), 125.73 (s), 123.85 (s), 122.45 (s), 120.55 (t, *J* = 9.0 Hz), 114.70 (s), 112.10 (s), 110.58 (s).

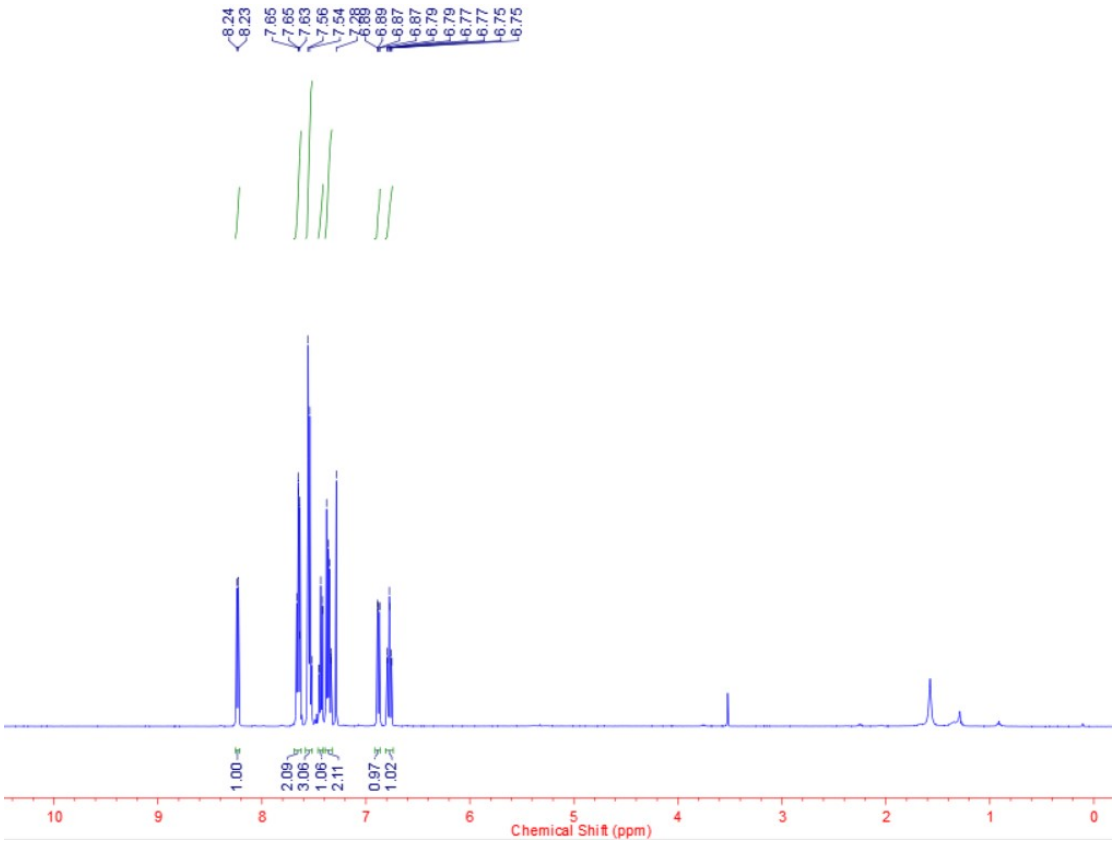

Fig. S1. ^{1}H NMR spectrum of **NPh_2FCz**.

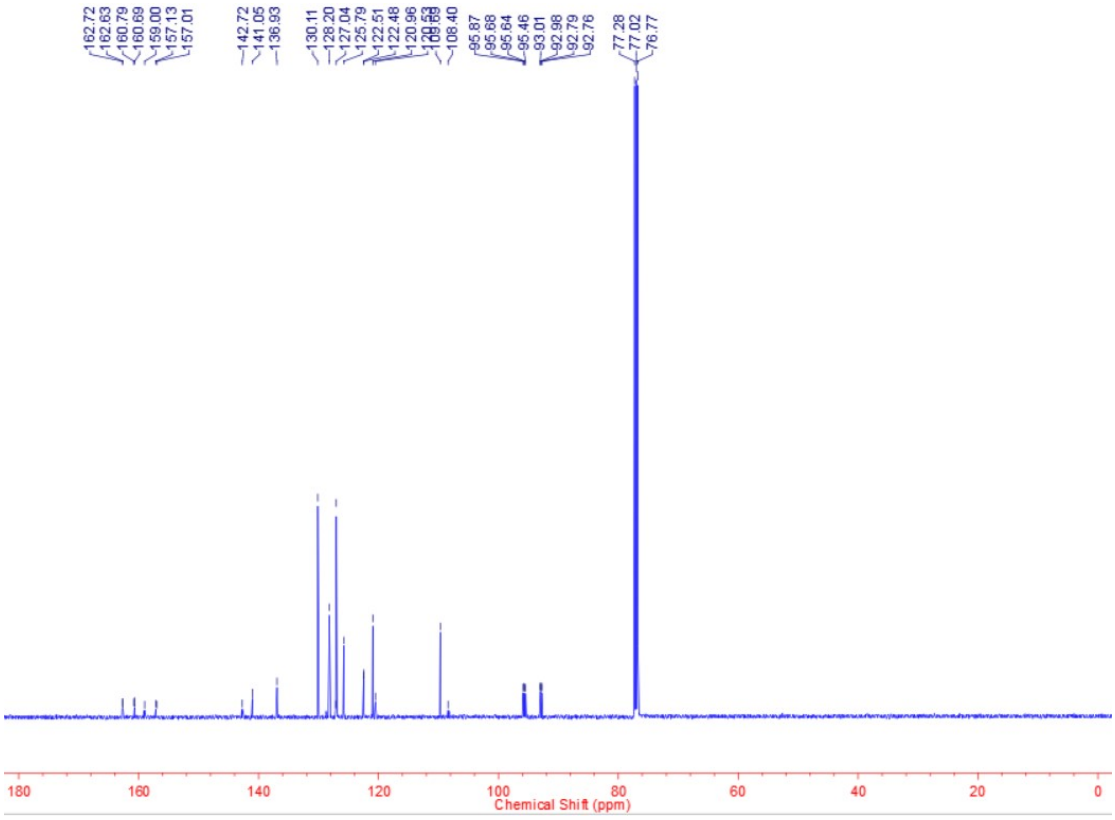

Fig. S2. ^{13}C NMR spectrum of **NPh_2FCz**.

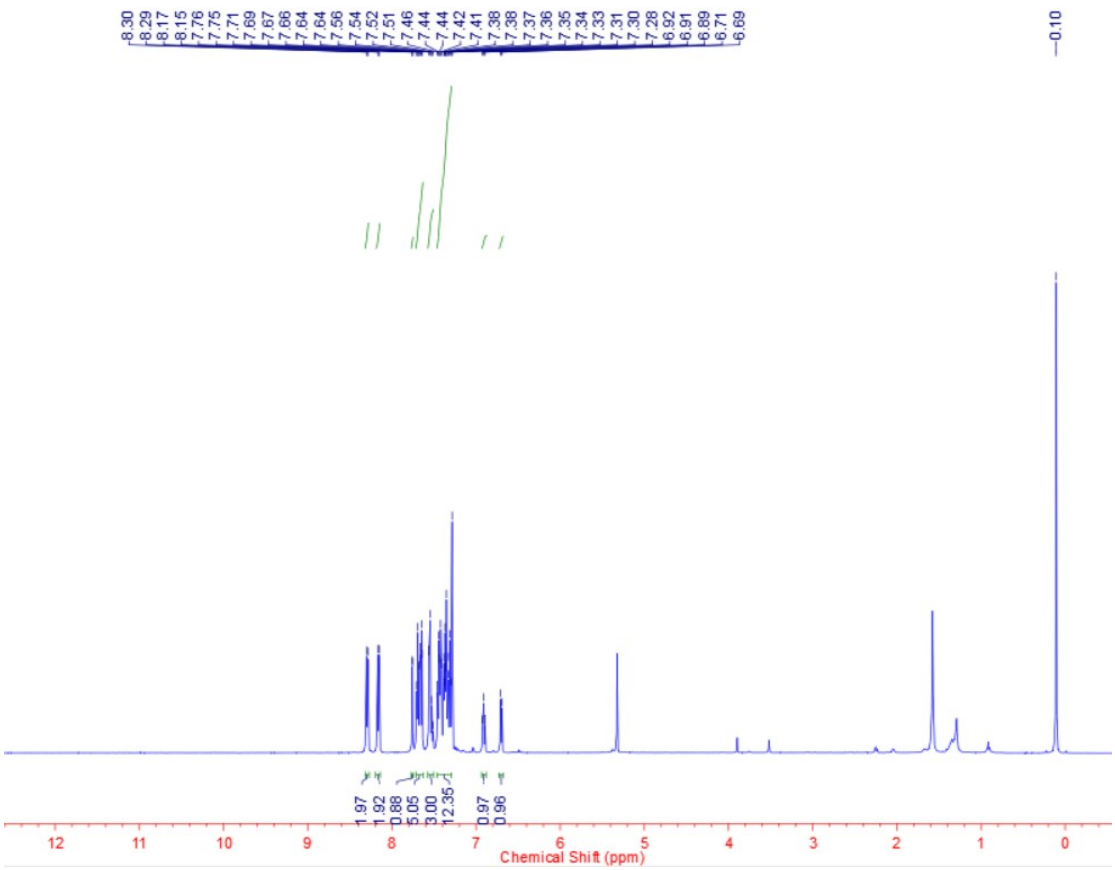

Fig. S3. ^{1}H NMR spectrum of **NPhCzDCz**.

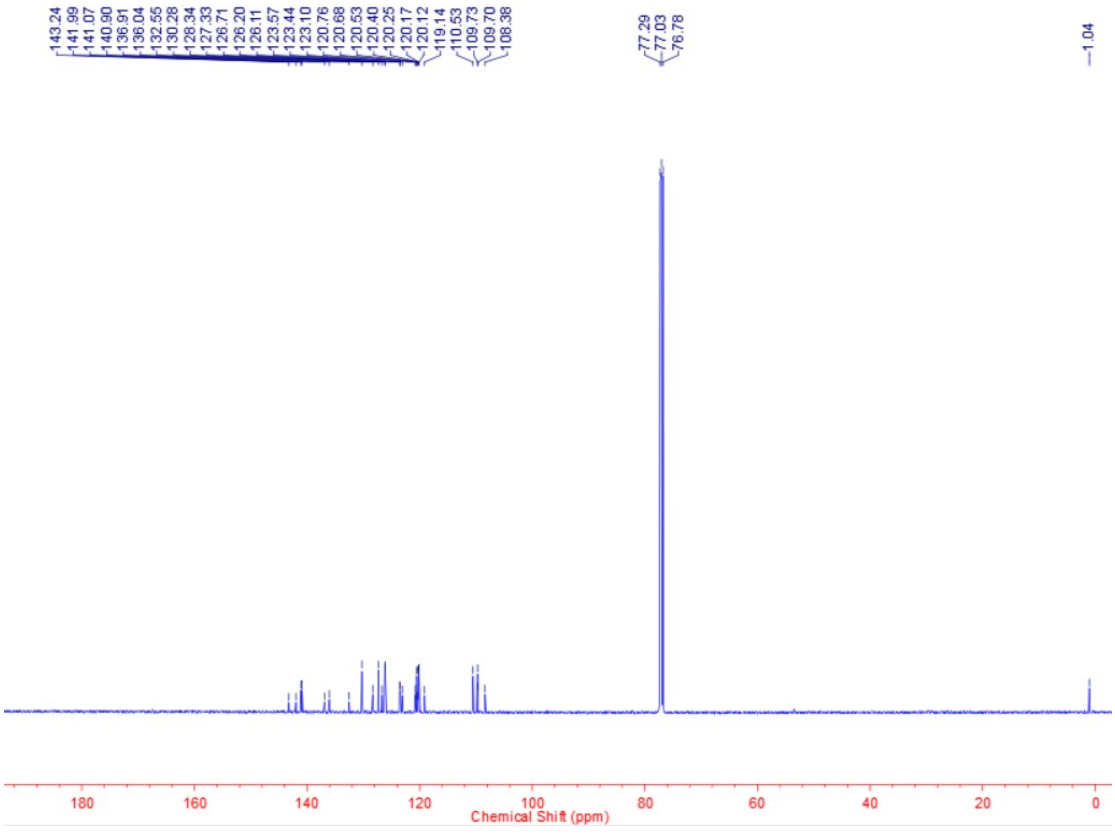

Fig. S4. ^{13}C NMR spectrum of **NPhCzDCz**.

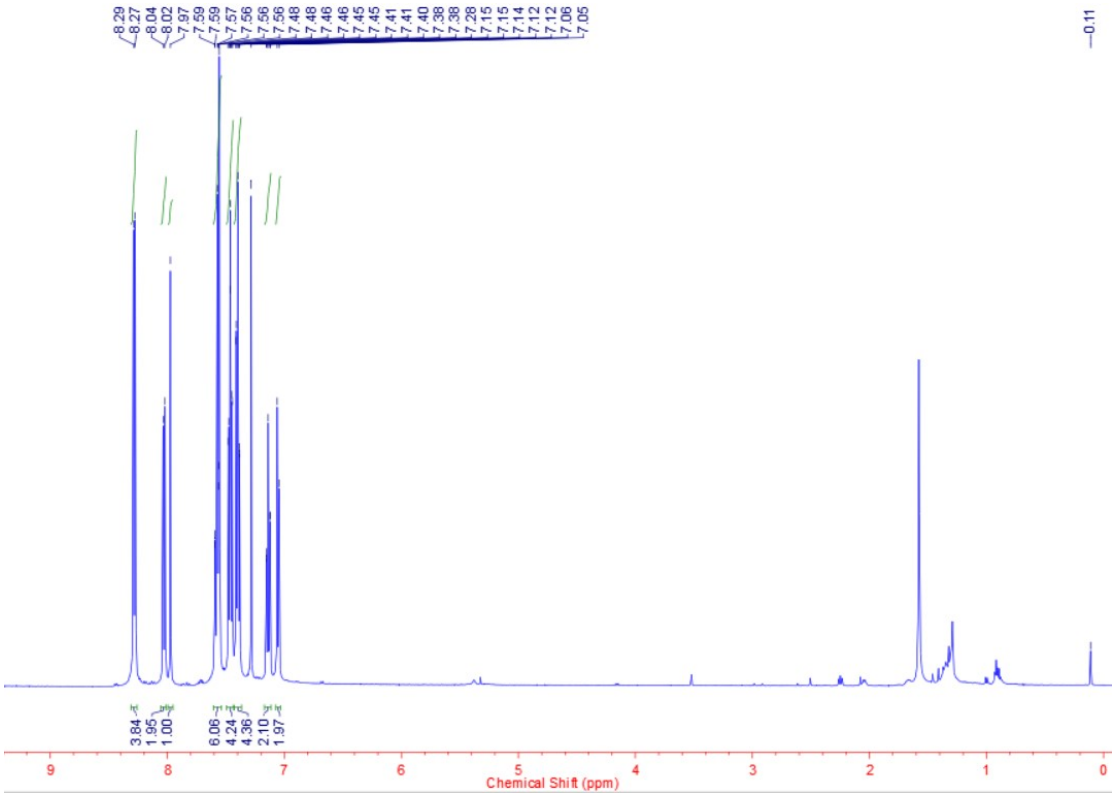

Fig. S5. ^{1}H NMR spectrum of **VTCzDCz**.

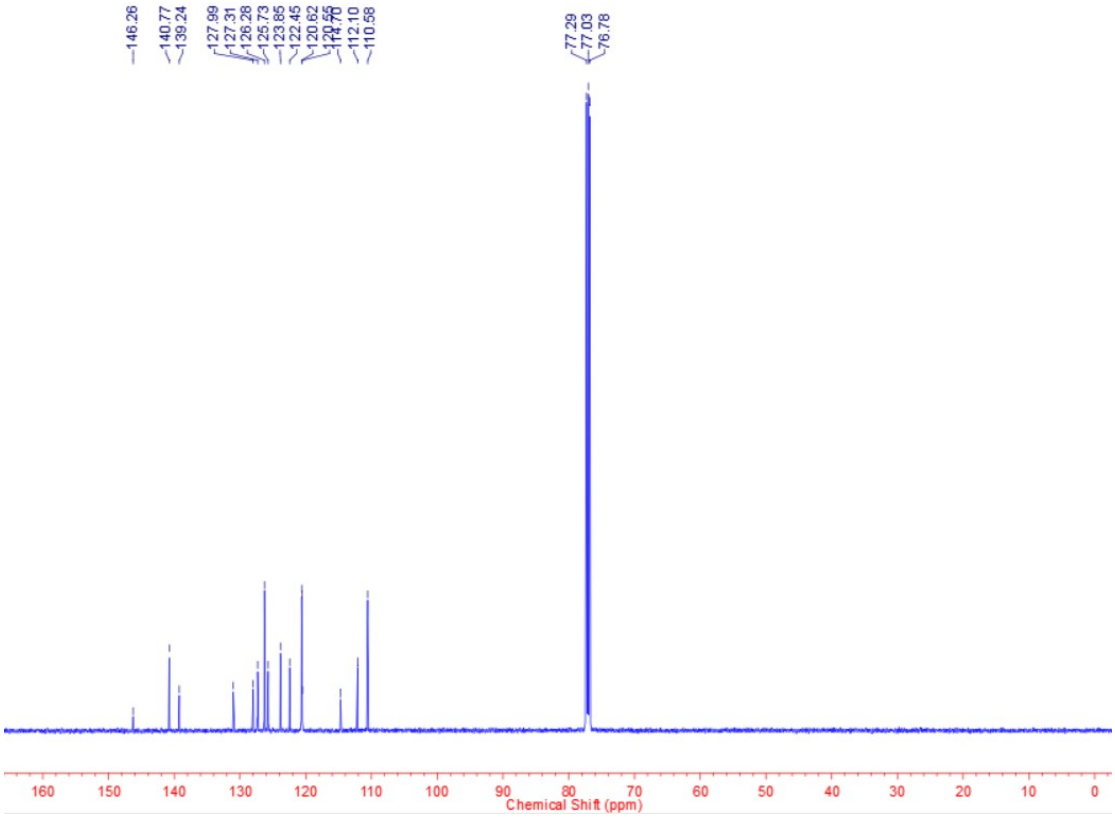

Fig. S6. ^{13}C NMR spectrum of **VTCzDCz**.

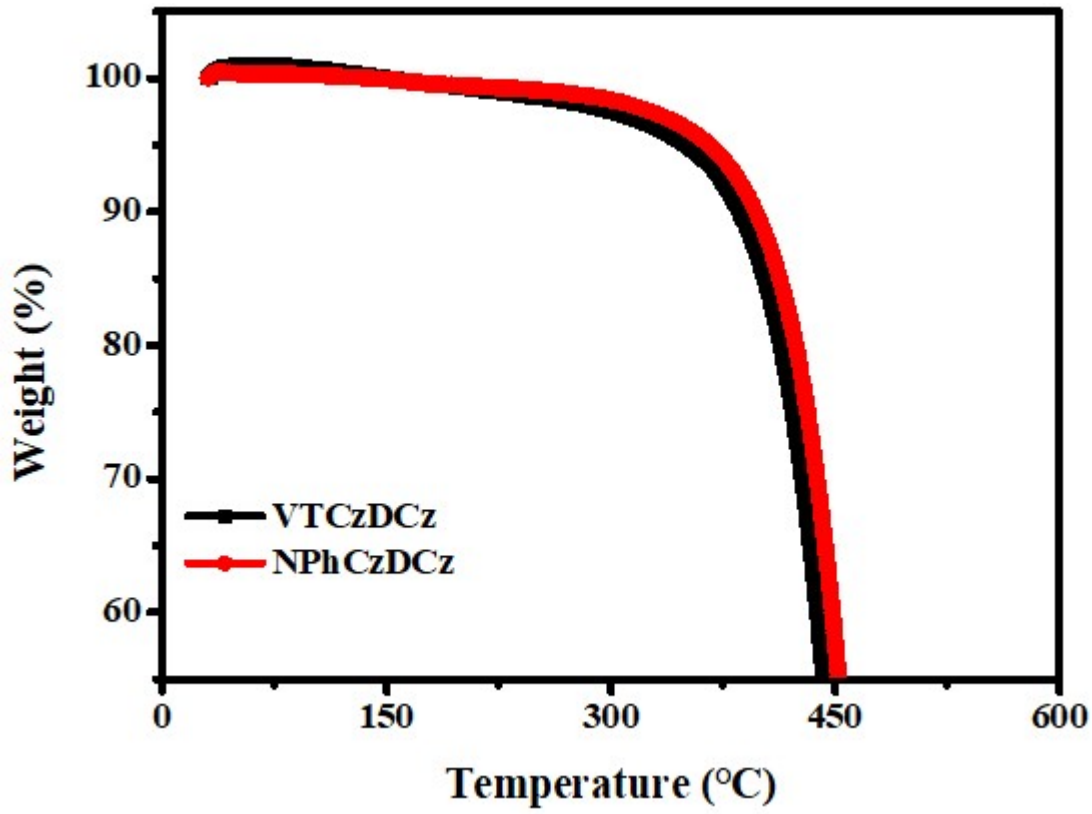

Fig. S7. Thermogravimetric analysis (TGA) curves of **VTCzDCz** and **NPhCzDCz**.

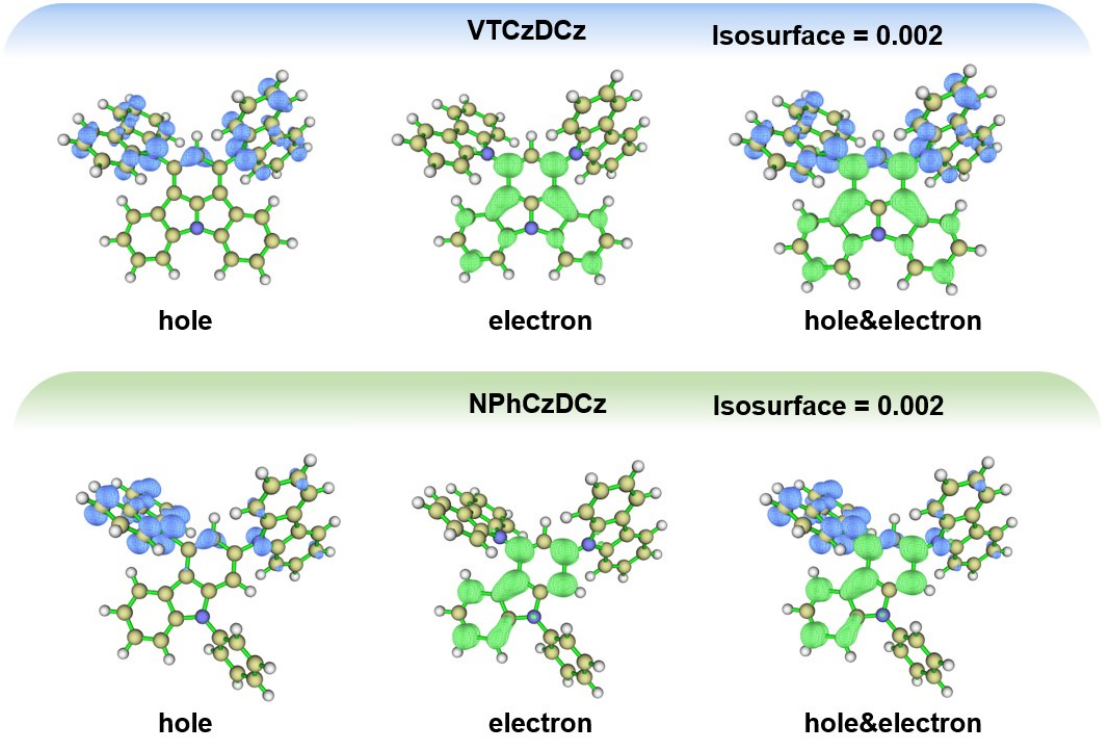

Fig. S8. Hole and electron distributions of both molecules.

Table S1. Summary of photophysical properties of NPhCzDCz and VTCzDCz.

Emitter	λ_{abs}[a] [nm]	λ_{fl}[a] [nm]	λ_{phos}[b] [nm]	E_S/E_T[c] [eV]	HOMO/LUMO [d] [eV]	T_d[e] [°C]
NPhCzDCz	320	379	434	3.27/2.86	-4.98/-1.65	362
VTCzDCz	350	404	469	3.07/2.64	-5.04/-1.91	343

[a]Measured in toluene solution (10^{-5} M) at room temperature; [b]Measured in toluene solution (10^{-5} M) at 77 K; [c]E_S/E_T: Singlet/triplet energies were calculated from onsets of the fluorescence and phosphorescence spectra in neat films at 77 K respectively; [d]HOMO and LUMO levels were calculated from CV data; [e]T_d: Decomposition temperature.

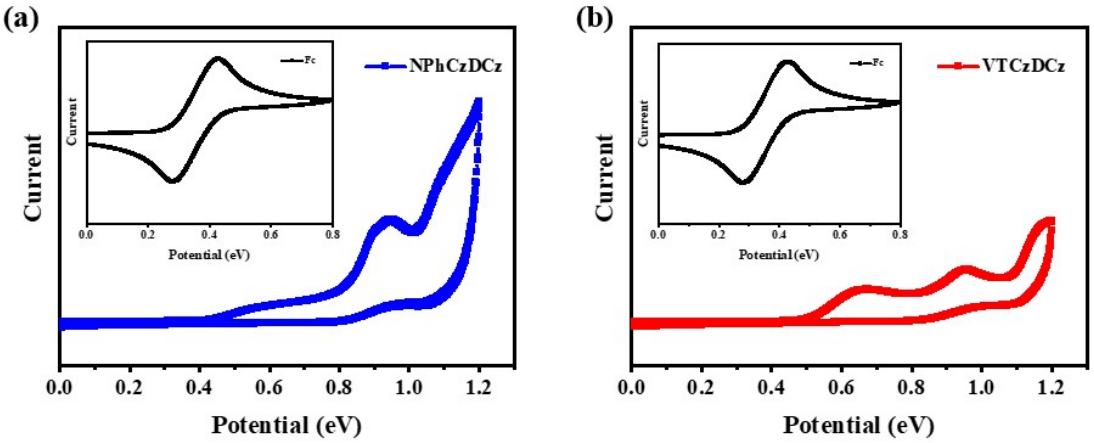

Fig. S9. Cyclic voltammogram curves of **VTCzDCz** and **NPhCzDCz** and **ferrocene** (inner illustration).

Table S2. Electrochemical properties of **VTCzDCz** and **NPhCzDCz**.

Molecule	$E_{ox,onset}$[a] (V)	$E_{g,opt}$[b] (eV)	E_{HOMO}[c] (eV)	E_{LUMO}[d] (eV)
VTCzDCz	0.66	3.13	-5.04	-1.91
NPhCzDCz	0.60	3.33	-4.98	-1.65

[a]The onset of oxidation curve; [b]Optical gap ($1240/\lambda_{onset}$); [c]E_{HOMO} = -[*E*ox - $E_{(Fc/Fc+)}$ + 4.8] eV; [d]E_{LUMO} =(E_{HOMO} + $E_{g,opt}$).

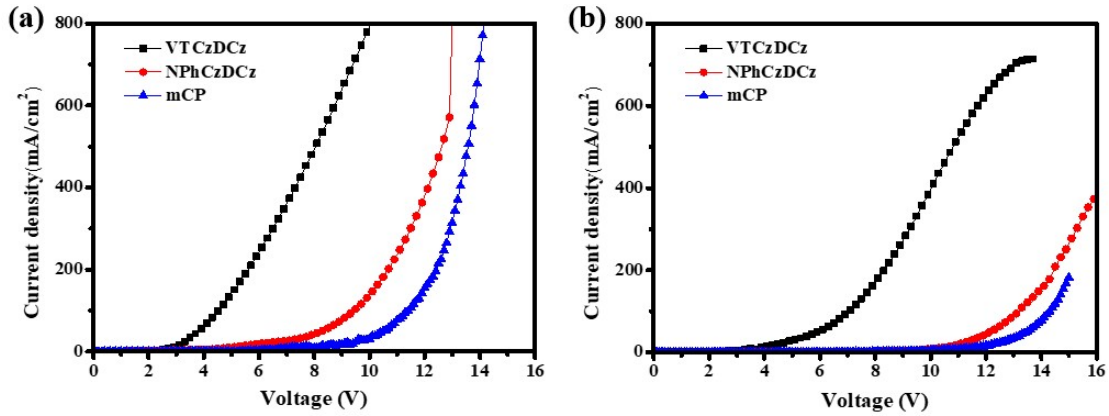

Fig. S10. Comparison of single-carrier devices based on VTCzDCz, NPhCzDCz, and mCP: (a) HOD; (b) EOD.

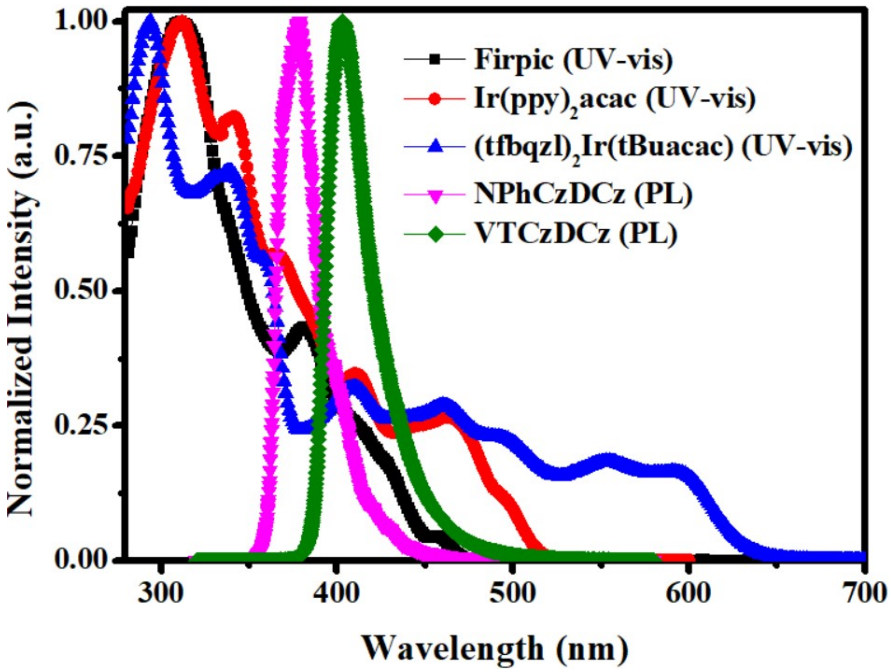

Fig. S11. The emission spectra of the two host materials and the UV-vis absorption spectra of the three phosphorescent materials.

Table S3. Crystallographic data of VTCzDCz.

	VTCzDCz
Moiety formula	$2(C_{42}H_{25}N_3)$, C_3H_7NO
FW	1216.40
Wavelength (Å)	0.71073
Crystal system	triclinic

Space group	*P* -1
a (Å)	12.6690(6)
b (Å)	14.2191(7)
c (Å)	17.5161(9)
α (deg)	90.205(2)
β (deg)	92.857(2)
γ (deg)	98.280(2)
V (Å^3)	3118.4(3)
Z	2
ρ_{calcd} (mg/cm^3)	1.296
μ (Mo Kα) (mm^{-1})	0.077
F (000)	1272.0
Reflns collected	9847
GOF on F^2	1.080
$R_1{}^a$, $wR_2{}^b$ [$I > 2\sigma(I)$]	0.0518, 0.1299
$R_1{}^a$, $wR_2{}^b$ (all data)	0.0834, 0.1451
CCDC NO	2365727

$R_1{}^a = \Sigma||F_o| - |F_c||/\Sigma|F_o|$. $wR_2{}^b = [\Sigma w(F_o{}^2 - F_c{}^2)^2/\Sigma w(F_o{}^2)]^{1/2}$

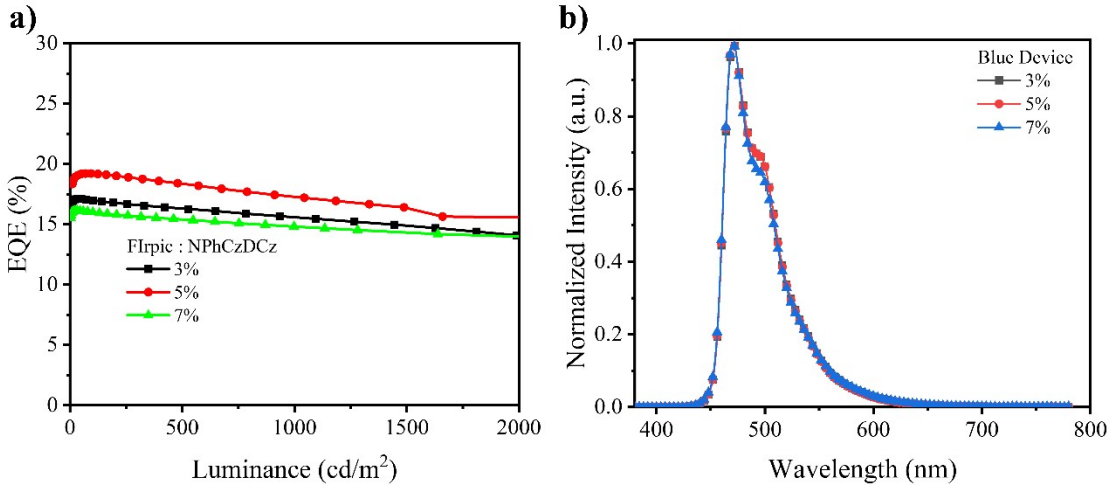

Figure S12. Blue device performances with different doping concentrations. a) EQE-luminance curves and b) EL spectra of blue PhOLEDs at 5V.

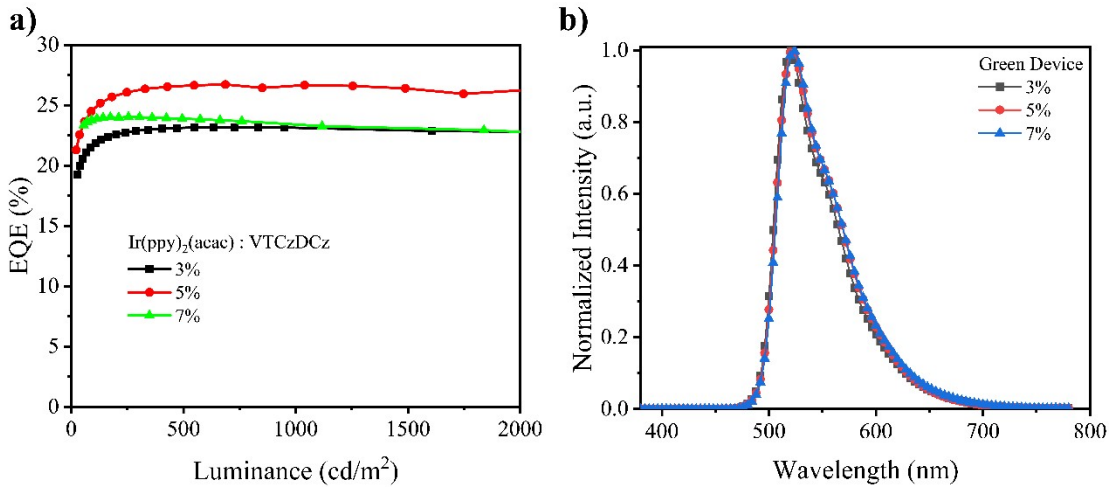

Figure S13. Green device performances with different doping concentrations. a) EQE-luminance curves and b) EL spectra of green PhOLEDs at 5V.

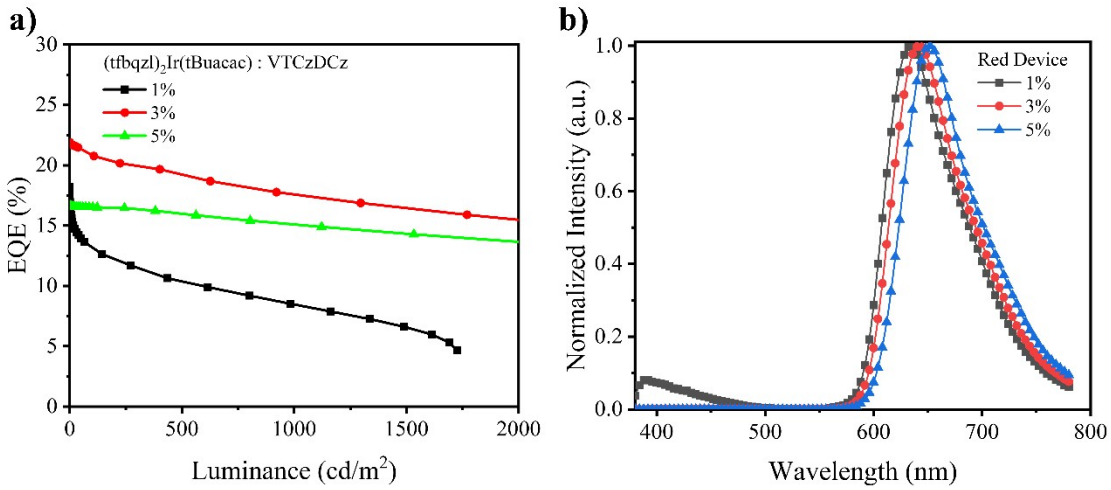

Figure S14. Red device performances with different doping concentrations. a) EQE-luminance curves and b) EL spectra of red PhOLEDs at 5V.

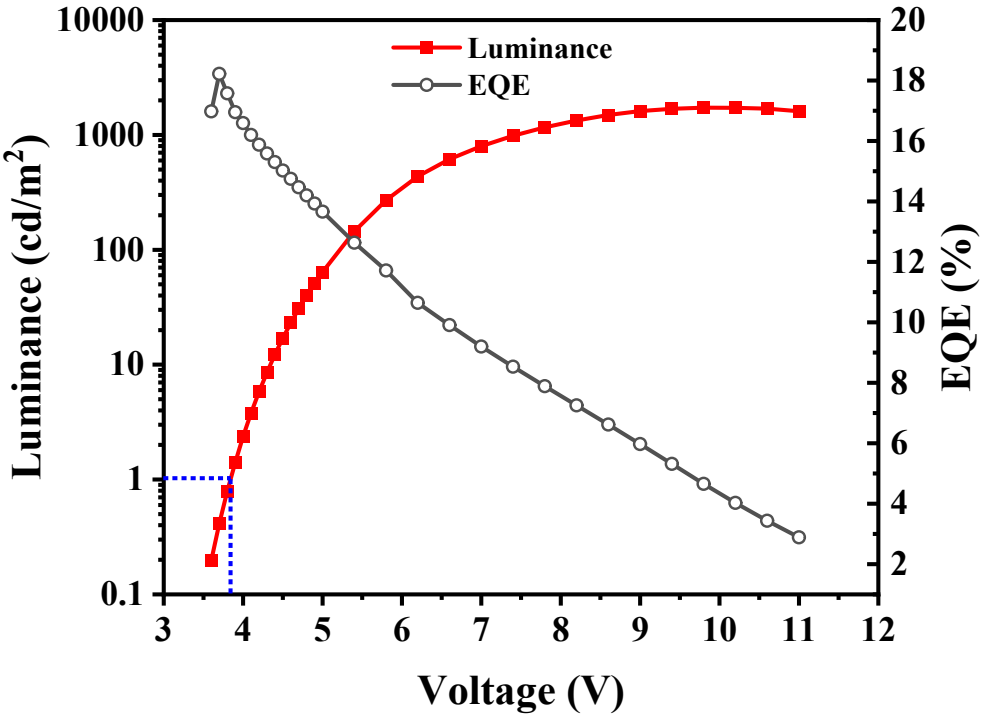

Figure S15. An EQE and luminance- voltage curve of red device.

Table S4. Electroluminescence characteristics of the optimized devices.

Device	Host	V_{on} [a] [V][b]	$CE_{max/100/1000}$[b] [cd A^{-1}]	$EQE_{max/100/1000}$[c] [%]	CIE [d] [x, y]
Blue	mCP	4.5	27.8/19.7/15.7	14.9/10.8/8.3	0.15, 0.30
	NPhCzDCz	3.4	35.8/35.6/31.9	19.2/19.1/17.2	0.15, 0.31
Green	mCP	4.0	72.9/48.5/32.9	20.1/13.4/9.1	0.31, 0.63
	NPhCzDCz	3.3	79.6/78.1/77.6	22.0/21.5/21.4	0.33, 0.63
	VTCzDCz	3.2	98.0/92.2/97.0	26.7/25.2/26.4	0.33, 0.63
Red	mCP	4.1	6.8/4.5/3.6	15.5/10.3/7.8	0.70, 0.30
	NPhCzDCz	4.0	9.3/7.8/6.4	19.5/16.0/12.9	0.70, 0.30

	VTCzDCz	4.1	12.2/11.7/10.1	21.9/20.8/17.8	0.69, 0.31

[a] Voltages at 1 cd m^{-2}; [b] The maximal current efficiency and at 100, and 1000 cd/m^2; [c] The maximal EQE and at 100, and 1000 cd/m^2; [d] Commission International de I'Eclairage coordinates.